Retrieval of an induced magnetic field in Mars ionosphere from Marsis data. Models and simulations

Salvador Jiménez[1], M. Ramírez-Nicolás[2], D. Usero[2], P.J. Pascual[3], M.P. Velasco[1], L. Vázquez[2]

1 Universidad Politécnica de Madrid, 2 Universidad Complutense de Madrid, 3 Universidad Autónoma de Madrid, Spain.

February 28th 2018

This work partially supported by the Spanish Ministry under grants: AYA2011-29967-C05-02 and ESP2016-79135-R

Introduction

■ *"Estudios de la exploración de Marte"* a Spanish research group on Mars Studies.

- Scientific support for instruments in missions to Mars.
- Exploitation of data from space missions. Data mining.
- Modelling.
- Formation: PhD students.

■ International collaborations with other groups, within ESA, IKI, FMI...

⋆ Some results on the retrieval of information ⋆
⋆ on Mars Ionosphere from MARSIS ⋆

Dust-Devils detection by means of Tomography

C. Aguirre, Luis Vázquez, Rui Vilela-Mendes, Raquel Caro, María Ramírez-Nicolás

Universidad Autónoma de Madrid, Escuela Politécnica Superior, Spain., Universidad Complutense de Madrid, Facultad de Informática, Spain, Centro de Matemática e Aplicações Fundamentais, University of Lisbon C6 , Lisboa, Portugal.Universidad Pontificia Comillas de Madrid, Escuela Técnica Superior de Ingeniería - ICAI, Madrid, Spain.

Introduction

Dust devils are convective vortices generated due to surface heating, thereby generating convective plumes of rising air with a pressure variation inside. Some of these vortices obtain horizontal wind speeds large enough for dust particles to be lifted off the surface and into the vortex and thus becoming dust devils. For this study, the pressure data used are those obtained directly by NASA's Phoenix spacecraft.

We propose a new technique called Adapted Tomography, which is based on using an operator with the shape of the event we want to extract, and this will be identified as the component of the signal we want. This produces a localized accumulation of energy where

Tomography for signal analysis

Tomograms are strictly positive probability densities and provide a full characterization of the signal. Tomograms are obtained by projecting a given signal ***f(t)*** over the eigenvector set of a linear operator ***B(α)***. The time-frequency tomogram is defined in the following way:

$$\mu = \frac{\cos\theta}{T}, \quad \nu = \frac{\sin\theta}{\Omega}$$

Using the previously defined operators B(μ,ν)

Martian atmospheric dust dynamics: modeling and numerical computations

Velasco M.P.[1], Usero D.[2], Jiménez S.[1], Vázquez-Poletti J.L.[3], Vázquez L.[2]

(Authors thank the special support from the MINECO of Spain, projects ESP2016-79135-R, TIN2015-65469-P.)

1 Introduction

The scattering of the solar radiation by dust aerosols has a direct effect on both surface and atmospheric heating rates, which are also basic drivers of atmospheric dynamics, and this fact affects the behavior of the Martian atmosphere [1].

Under different Martian atmospheric scenarios, the measure of the amount of solar radiation at the Martian surface will be useful to gain some insight into the following issues:

1) UV irradiation levels at the bottom of the Martian atmosphere to use them as an habitability index.

2) Incoming shortwave radiation and solar heating at the surface.

3) Relative local index of dust in the atmosphere.

2 Modeling of the propagation of radiation in a medium

The attenuation of solar radiation traversing the atmosphere is modeled by the Lambert-Beer-Bouguer law, where the aerosol optical thickness plays a fundamental role. Ångstrm law [2] expresses the

3 Extension to 3D problem and numerical computation

The 1D model can be extended to full 3D:

$$\frac{\partial^\alpha \varphi}{\partial \lambda^\alpha} = \frac{\Gamma(\alpha+1)}{2\beta}\left(c_1\frac{\partial^2\varphi}{\partial x^2} + c_2\frac{\partial^2\varphi}{\partial y^2} + c_3\frac{\partial^2\varphi}{\partial z^2}\right), \qquad \alpha \in (0,1)\cup(1,2), \tag{10}$$

with an initial value problem and boundary conditions given by

$$\begin{cases} \lim_{\|\vec{x}\|\to\infty} \varphi(\lambda,\vec{x}) = 0, & \lambda > 0, \\ \varphi(0^+,\vec{x}) = g(\vec{x}), & \vec{x} \in \mathbb{R}^3, \\ \left.\frac{\partial}{\partial\lambda}\varphi(\lambda,\vec{x})\right|_{\lambda=0} = 0 & \text{(additional condition when } 1 < \alpha < 2), \end{cases} \tag{11}$$

where $\vec{x} = (x,y,z)$, and coefficients c_j, $j = 1,2,3$, taken as constants, correspond to possible

Mars Express and MARSIS

- The first **ESA** mission to another planet.
- Launched, June 2, 2003, from Baikonur on a Russian Союз/Фрегат rocket.
- Martian orbit on December 20, 2003.
- May 4–10, 2005, deployment of MARSIS antenna.
- July 2005–present, nominal science observations.

[logo, www.esa.int]

- **MARSIS**: **M**ars **A**dvanced **R**adar **S**ubsurface and **I**onospheric **S**ounding. [1]
  - Primary goal: to probe for water below the surface of the planet.
  - Secondary goal: to measure the response of the ionosphere.
    AIS mode: **A**ctive **I**onospheric **S**ounding.
    Effective sounding of the ionosphere from the height of the spacecraft until the region with maximum density of the plasma.

Ionosphere and ionograms

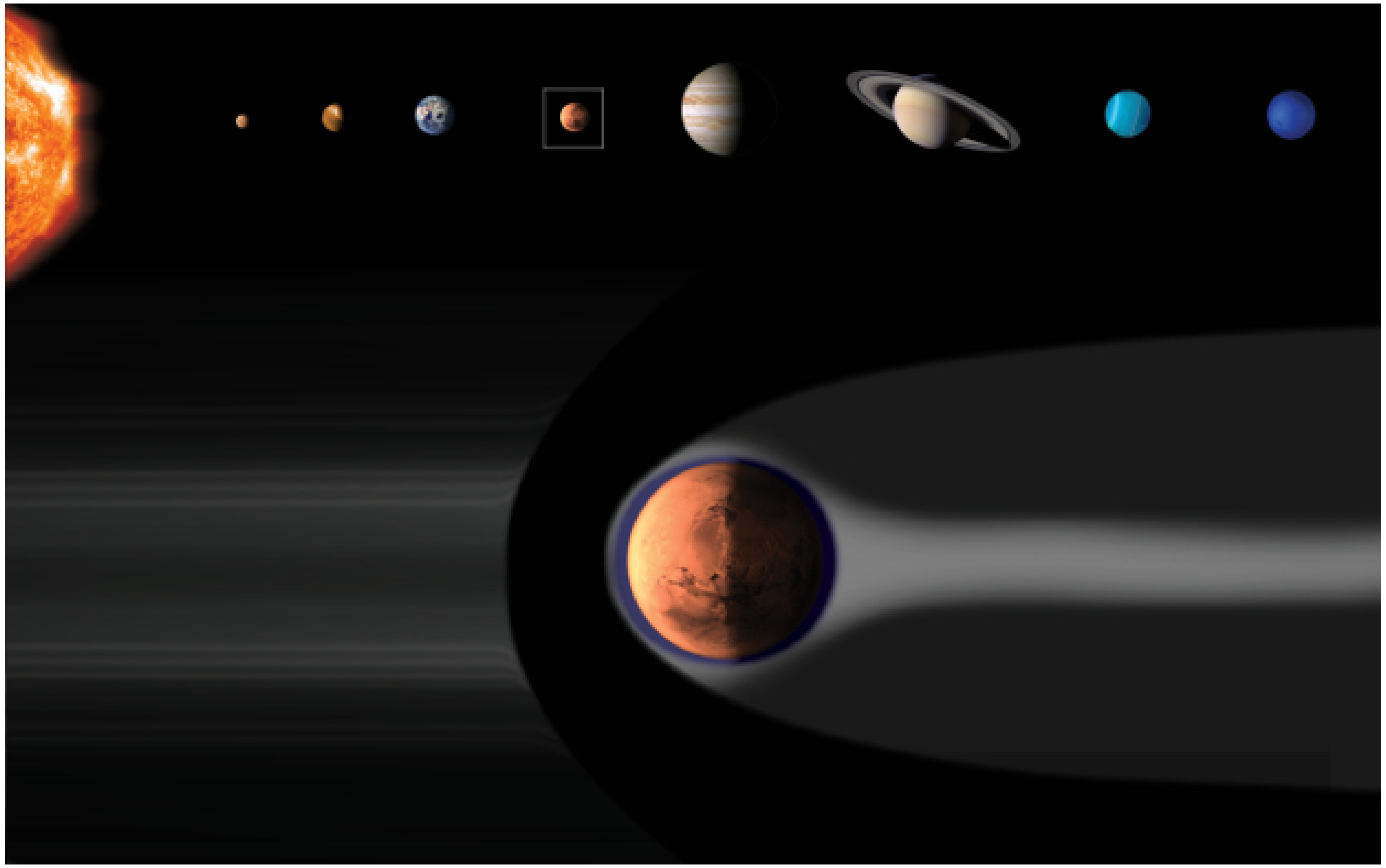

[Magnetosphere, www.esa.int]

Ionosphere

- plasma (electrons, ionized atoms or molecules...) around the planet.
- Boundary between lower atmosphere and the Solar wind.
- Two layers: M2 produced by the Solar EUV photons ($\lambda \sim$ 10nm–124nm), M1 produced by soft X-ray photons ($\lambda \sim$ 0.2nm–10nm).

- Stronly influenced by both the Solar wind (including **SZA**) and the crustal magnetic field on the planet (see [2], and references therein).

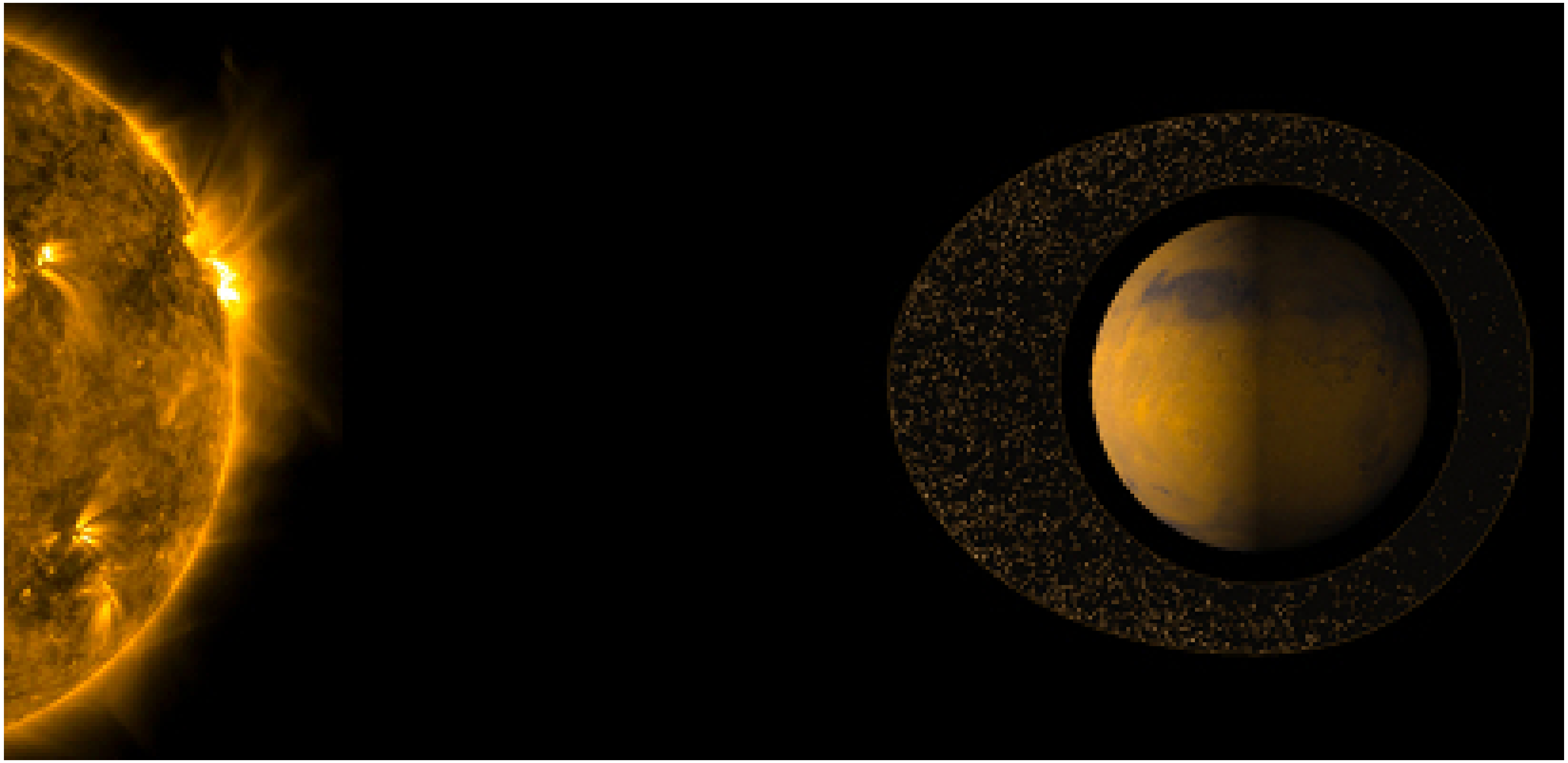

[representation of the response of the ionosphere to direct Solar irradiance. www.esa.int]

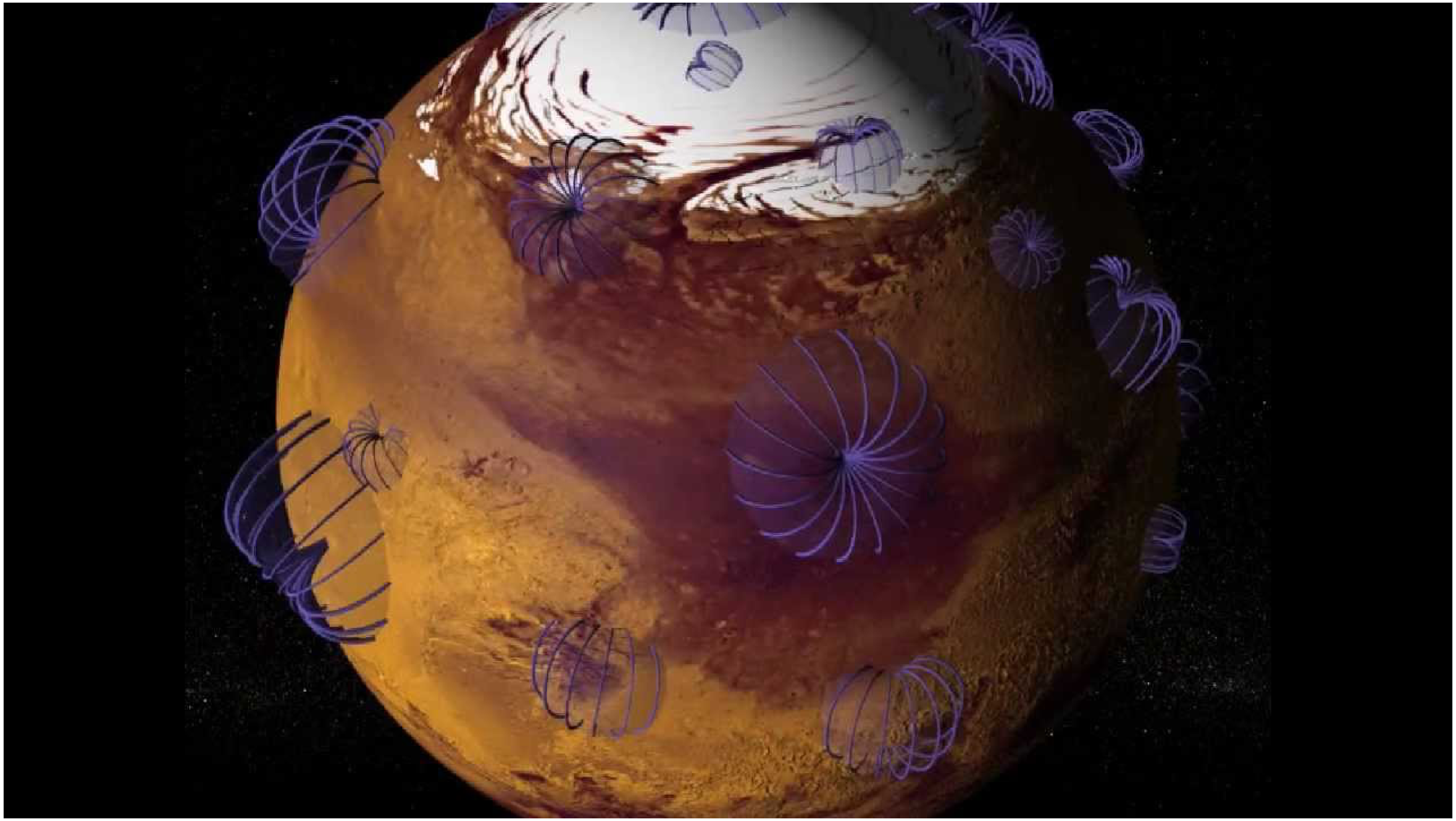

[Crustal magnetic field and its projection from the planet. www.esa.int]

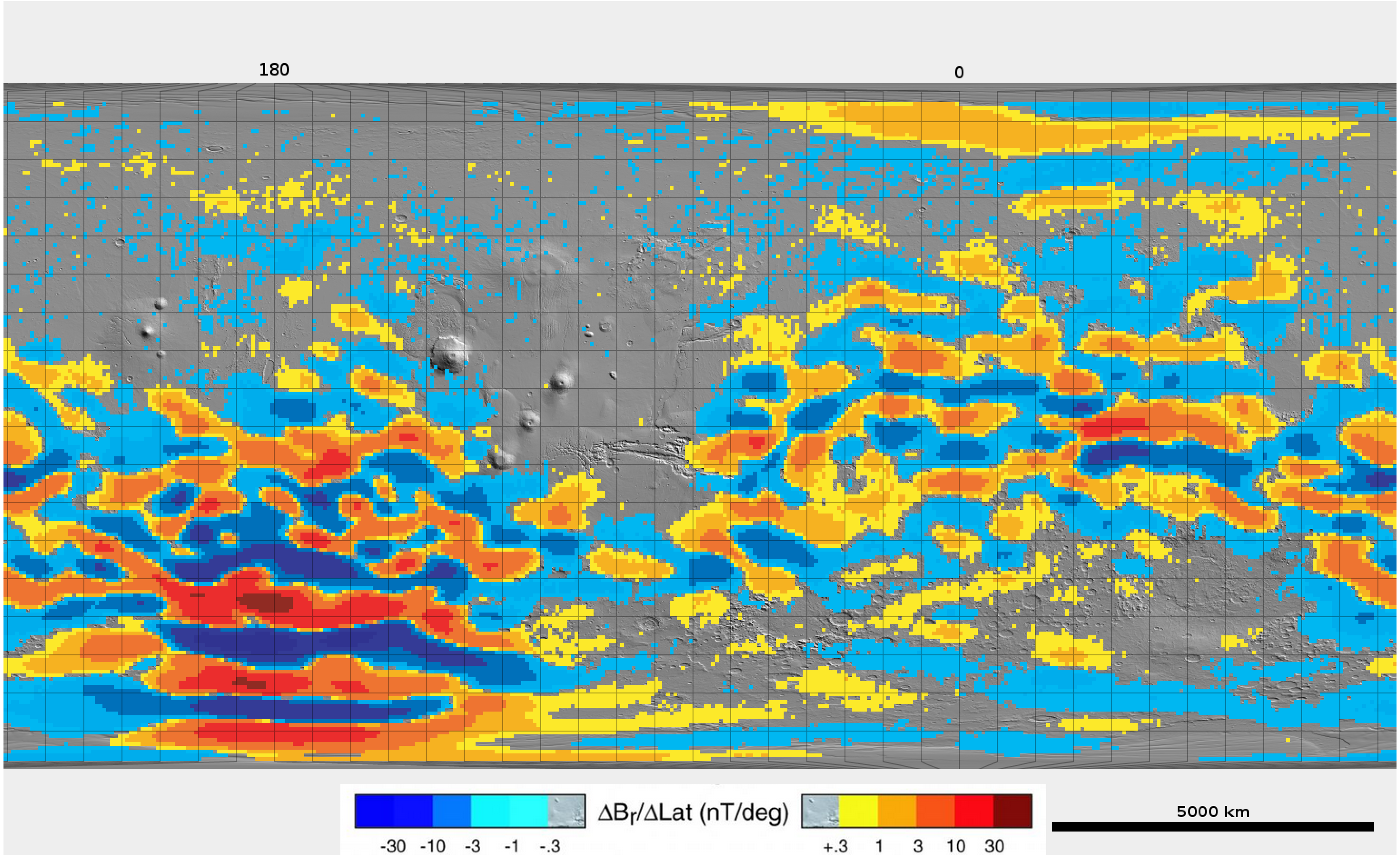

[intensity of the radial magnetic field on Mars. JMARS - MAG/ER instrument results]

Ionograms (see [3], and references therein)

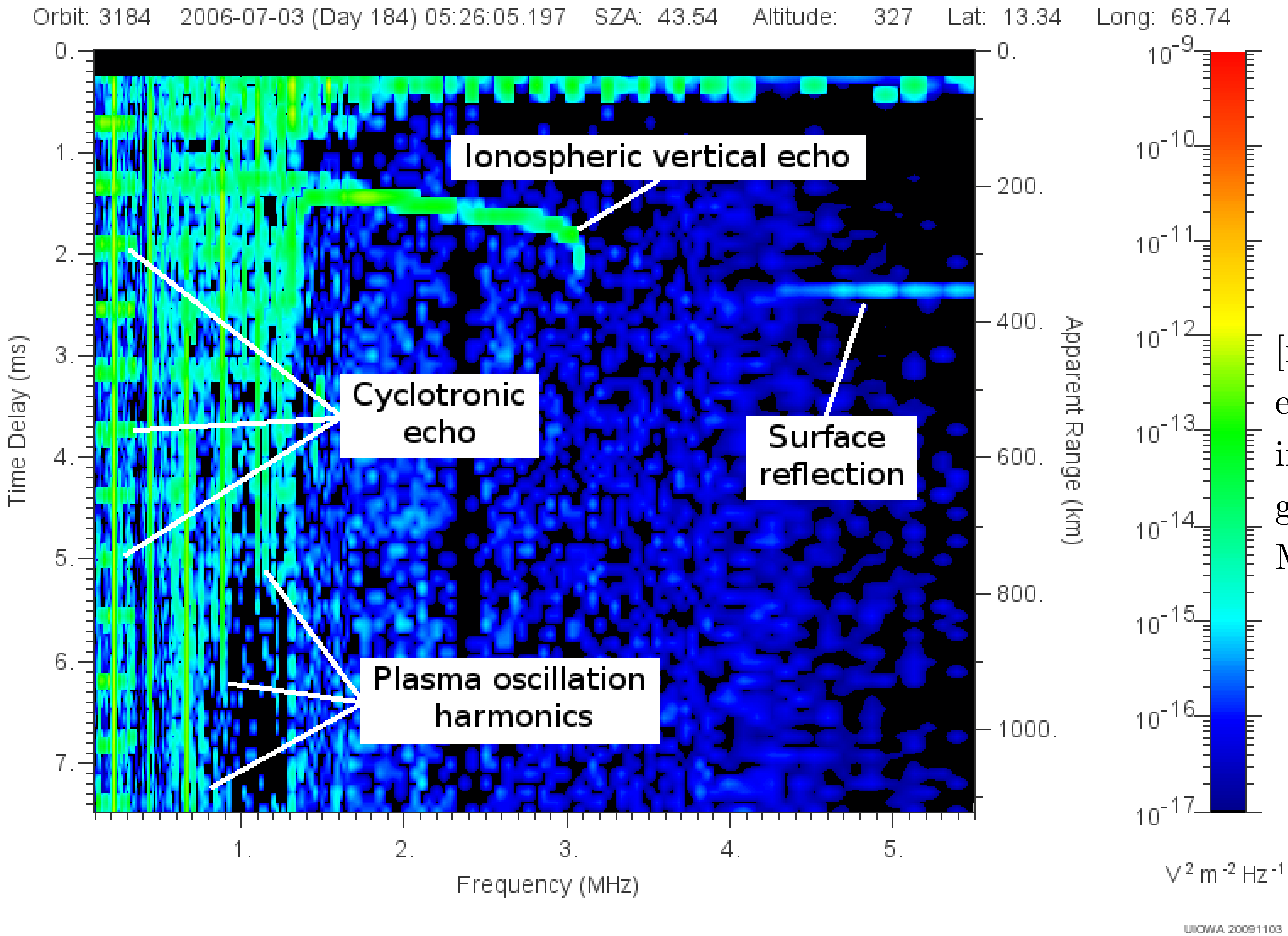

[main elements in a ionogram. MARSIS]

- Produced by the AIS mode with the radar sounding towards the planet
- The echos received back are represented versus the carrier frequency.
- The total time span for a ionogram is 1.26s, and an ionogram is recorded every 7.54s

Limitations:

- Mars Express has a highly excentrical elliptic orbit around Mars with a periapsis of 295Km and an apoapsis of 11000Km. Due to signal to noise ratio, AIS is only effective for heights below 1200Km, $\sim$ 40 min.
- This 40 min time-span is divided among the two modes: $\sim$10 min for AIS, $\sim$280 ionograms per orbit.
- Not all the ionograms recorded collect data with the information necessary to deduce the vertical electron profile nor the intensity of magnetic field at the spaceraft height.

⋆ **No trace of a magnetic field can be detected at spacecraft height (even if there is one there) unless a cloud of electrons surrounds the antenna**, since the intensity of the field is inferred from the cyclotron movements induced by the electrical field of the antenna on the electrons.

Modelling: [2]

• A time delay measures twice the time that it takes to a signal, travelling at the speed of light c, to reach the point where it is reflected.
• The time delays depend on the depth the signal penetrates down and are, thus, frequency dependent.
• Integrating over that distance (converting velocities into frequencies) we have:

$$\Delta t(f_{\mathrm{w}}) = \frac{2}{c}\int_{z_{\mathrm{refl}}}^{z_{\mathrm{sc}}} \frac{dz}{\sqrt{1-(f_{\mathrm{p}}(z)/f_{\mathrm{w}})^2}},$$

where f_{w} is the frequency of the signal, z_{refl} and z_{sc} the height where the reflection takes places and that of the spacecraft, respectively, and f_{p} is the plasma frequency.

This corresponds to Abel's integral equation, with solution formaly given by:

$$z_{\mathrm{refl}}(f_{\mathrm{p}}) = \frac{c}{\pi} \int_{\alpha_0}^{\pi/2} \Delta t\left(f_{\mathrm{p}} \sin\alpha\right)\, d\alpha,$$

where the auxiliary variables α and α_0 are such that

$$\sin\alpha = \frac{f_{\mathrm{w}}}{f_{\mathrm{p}}}, \sin\alpha_0 = \frac{f_{\mathrm{p}}(z_{\mathrm{sc}})}{f_{\mathrm{p}}}.$$

Different aspects have to be taken into consideration:

- Noise.
- Uncertainty on the height of the spacecraft.
- Precision of the measurements.
- Retrieval of values from the ionograms.

As a result the electronic density at the different heights can be estimated, giving the vertical electron profile for a given orbit [2].

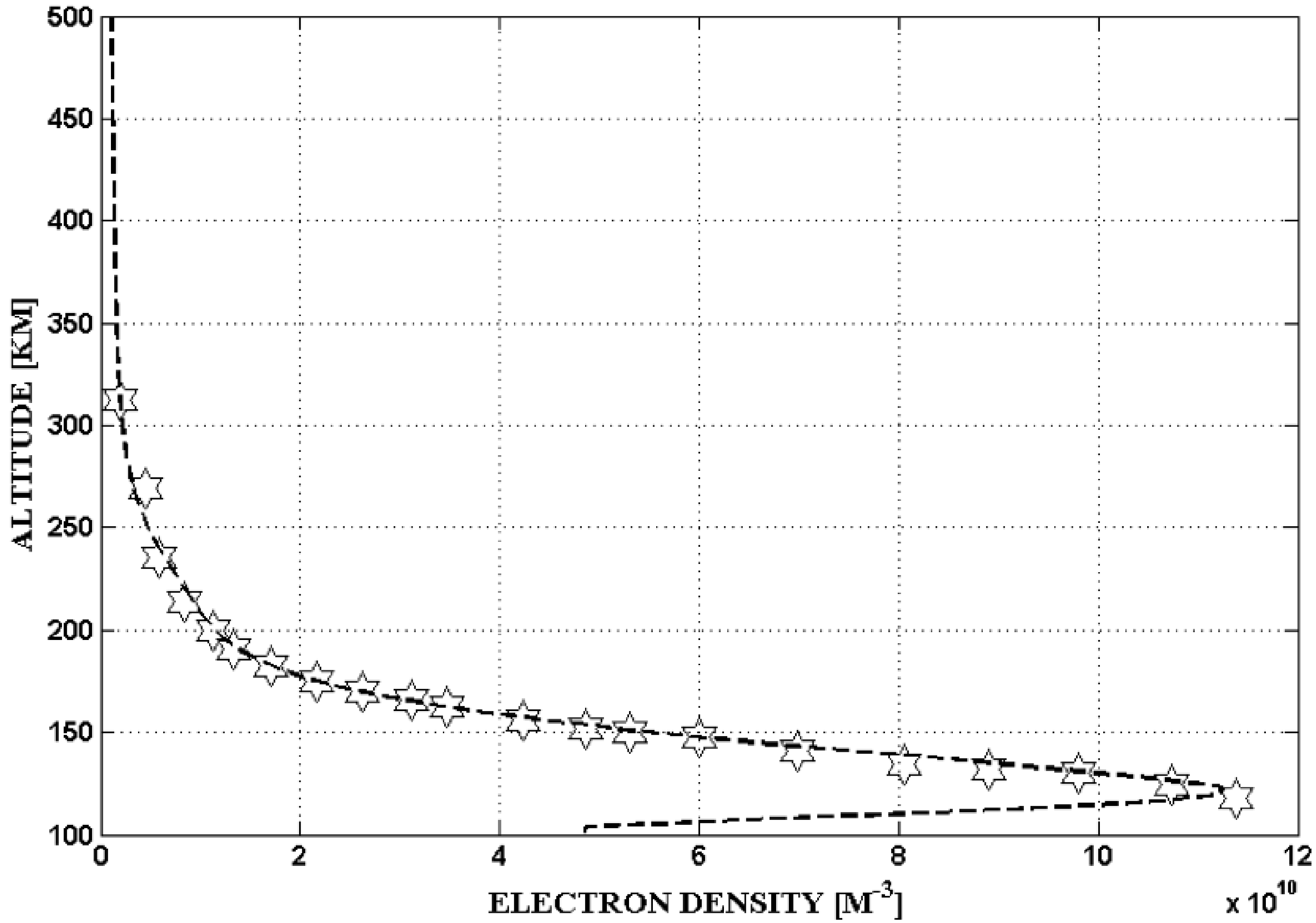

[comparison of the data obtained with a numerical model of Mars atmosphere.[2]]

The magnetic field can be obtained from the equations of the dynamics of the electrons in the presence of the magnetic field near the antenna

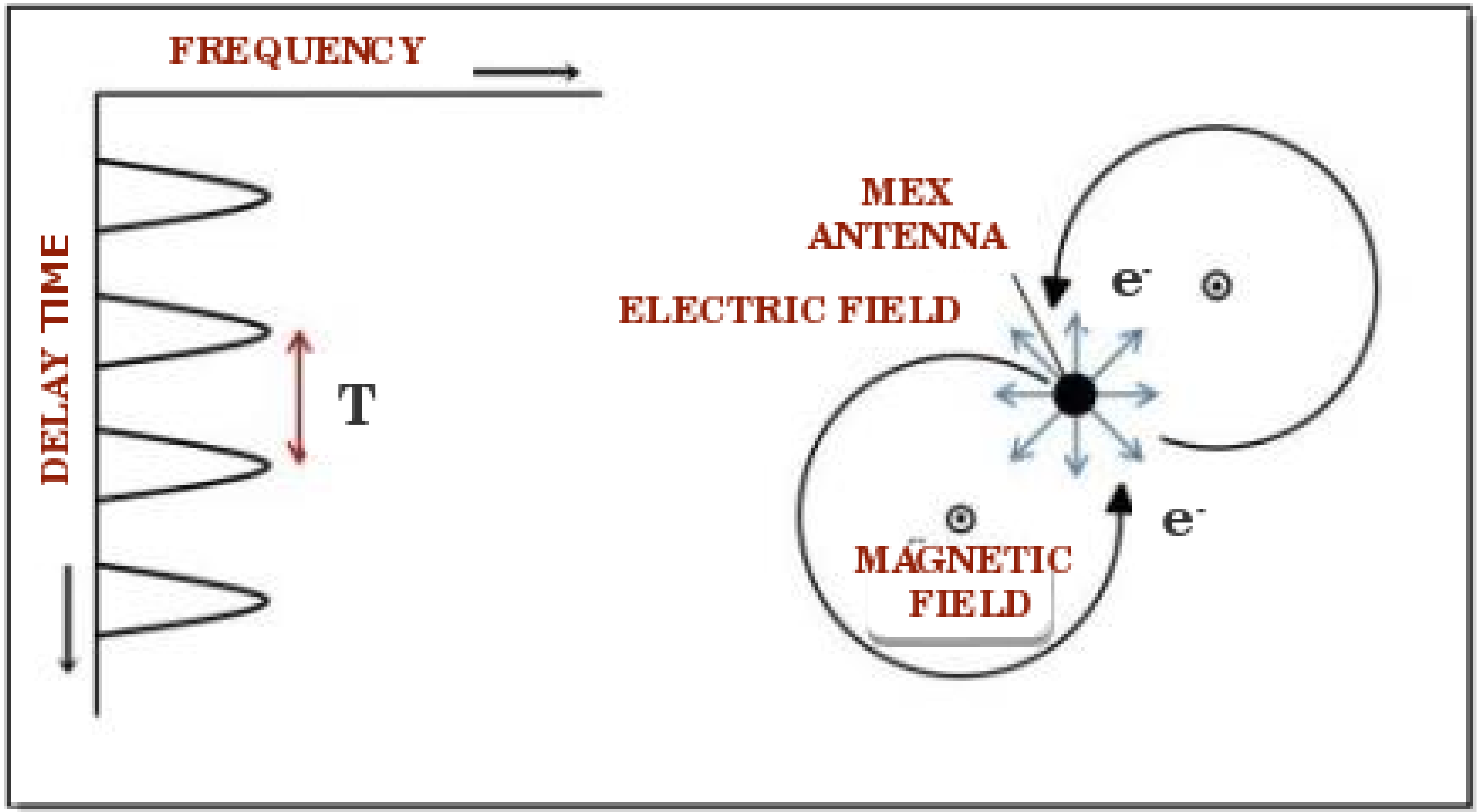

[scheme of the movement of the electrons near MARSIS antenna.[2]]

From the Lorenz force and Newton second law we obtain [4]:

$$B = \frac{m}{e \sin \alpha} \frac{2\pi}{T}.$$

where B is the modulus of the magnetic field, m and e, respectively, the mass and the charge of the electron, T the period of the cyclotronic movement around the antenna and α the angle with respect to the field (supposed to be 90°).

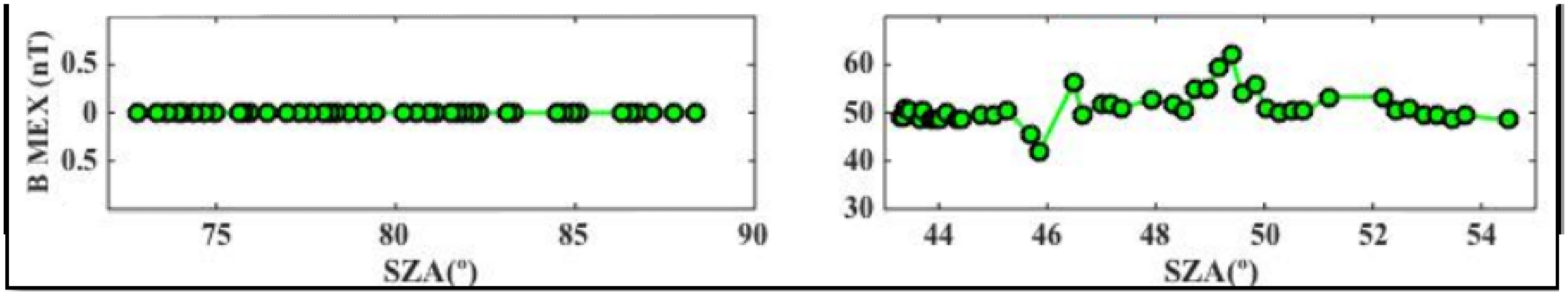

[B for two different orbits of Mars Express as a function of the Solar Zenital Angle.[2]]

First results:

Our aim is to process all ionograms from MARSIS in an automatic way as mentioned in Prof. Vázquez-Polletti et al. poster:

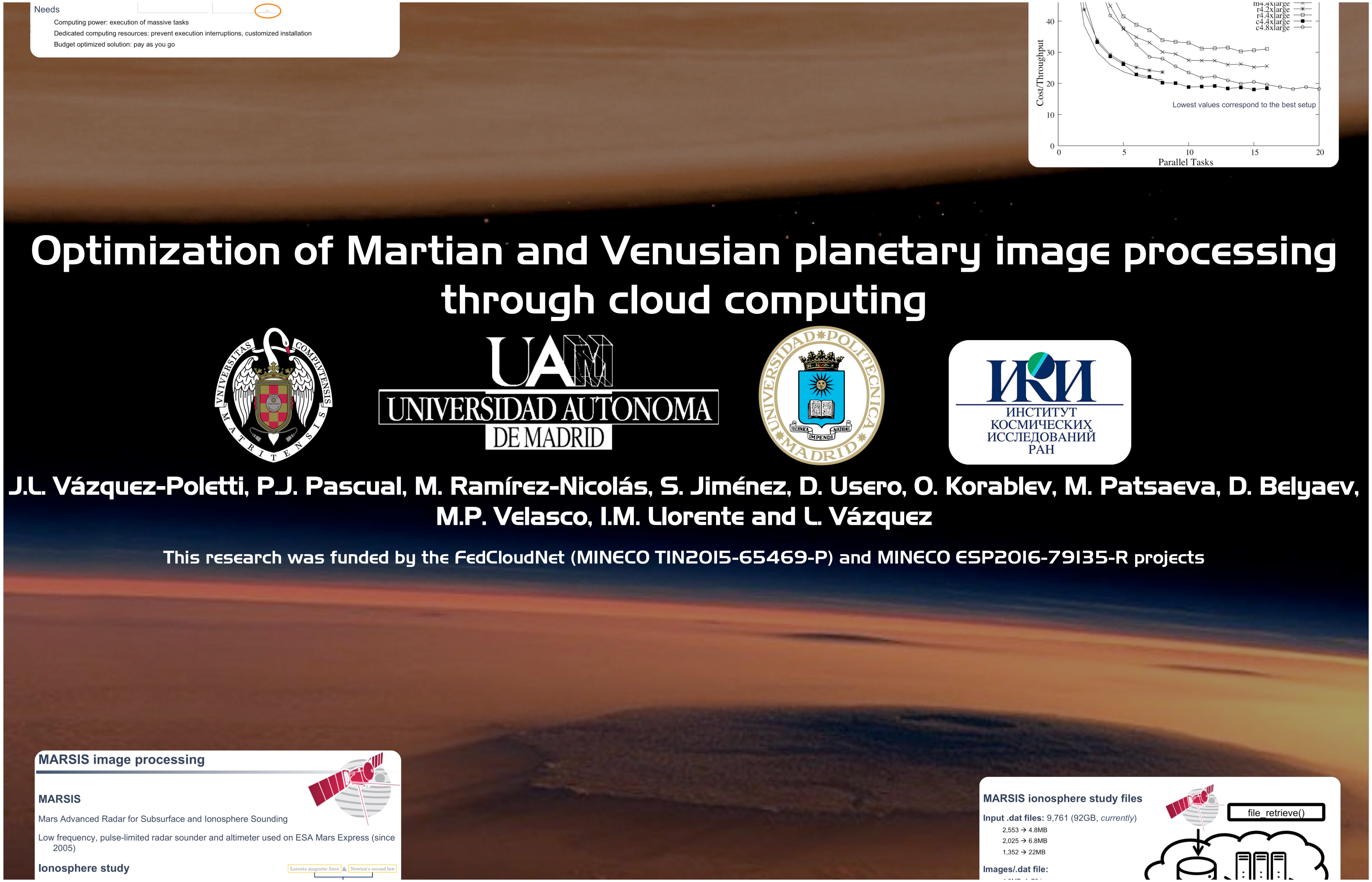
Needs
Computing power: execution of massive tasks
Dedicated computing resources: prevent execution interruptions, customized installation
Budget optimized solution: pay as you go
Cost/Throughput
Parallel Tasks
Lowest values correspond to the best setup
Optimization of Martian and Venusian planetary image processing through cloud computing
UNIVERSIDAD AUTONOMA DE MADRID
ИНСТИТУТ КОСМИЧЕСКИХ ИССЛЕДОВАНИЙ РАН
J.L. Vázquez-Poletti, P.J. Pascual, M. Ramírez-Nicolás, S. Jiménez, D. Usero, O. Korablev, M. Patsaeva, D. Belyaev, M.P. Velasco, I.M. Llorente and L. Vázquez
This research was funded by the FedCloudNet (MINECO TIN2015-65469-P) and MINECO ESP2016-79135-R projects
MARSIS image processing
MARSIS
Mars Advanced Radar for Subsurface and Ionosphere Sounding
Low frequency, pulse-limited radar sounder and altimeter used on ESA Mars Express (since 2005)
Ionosphere study
MARSIS ionosphere study files
Input .dat files: 9,761 (92GB, currently)
2,553 → 4.8MB
2,025 → 6.8MB
1,352 → 22MB
Images/.dat file:
file_retrieve()

Data from: 2005-175T18:19:27.689 to: 2011-365T23:16:02.529 (about 150,000 useful orbits)

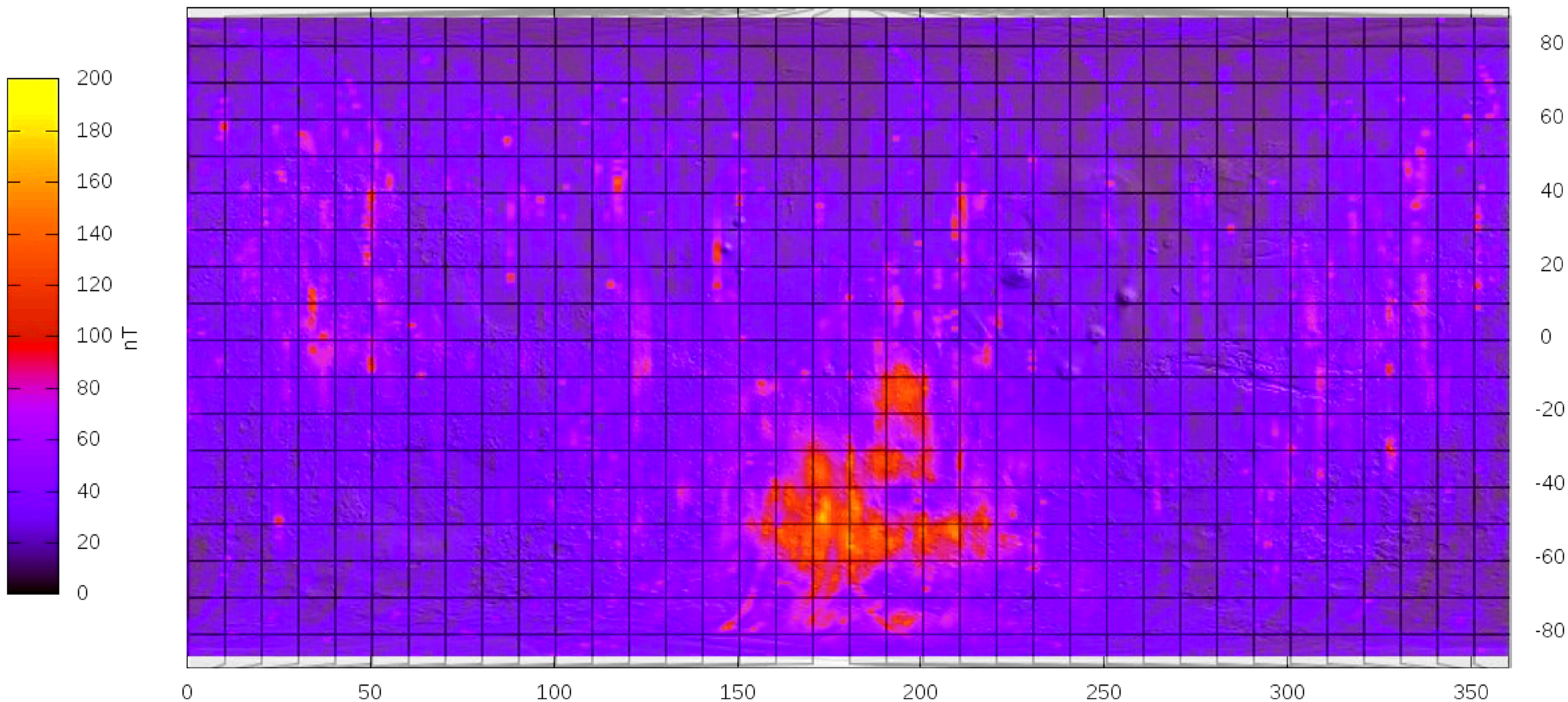

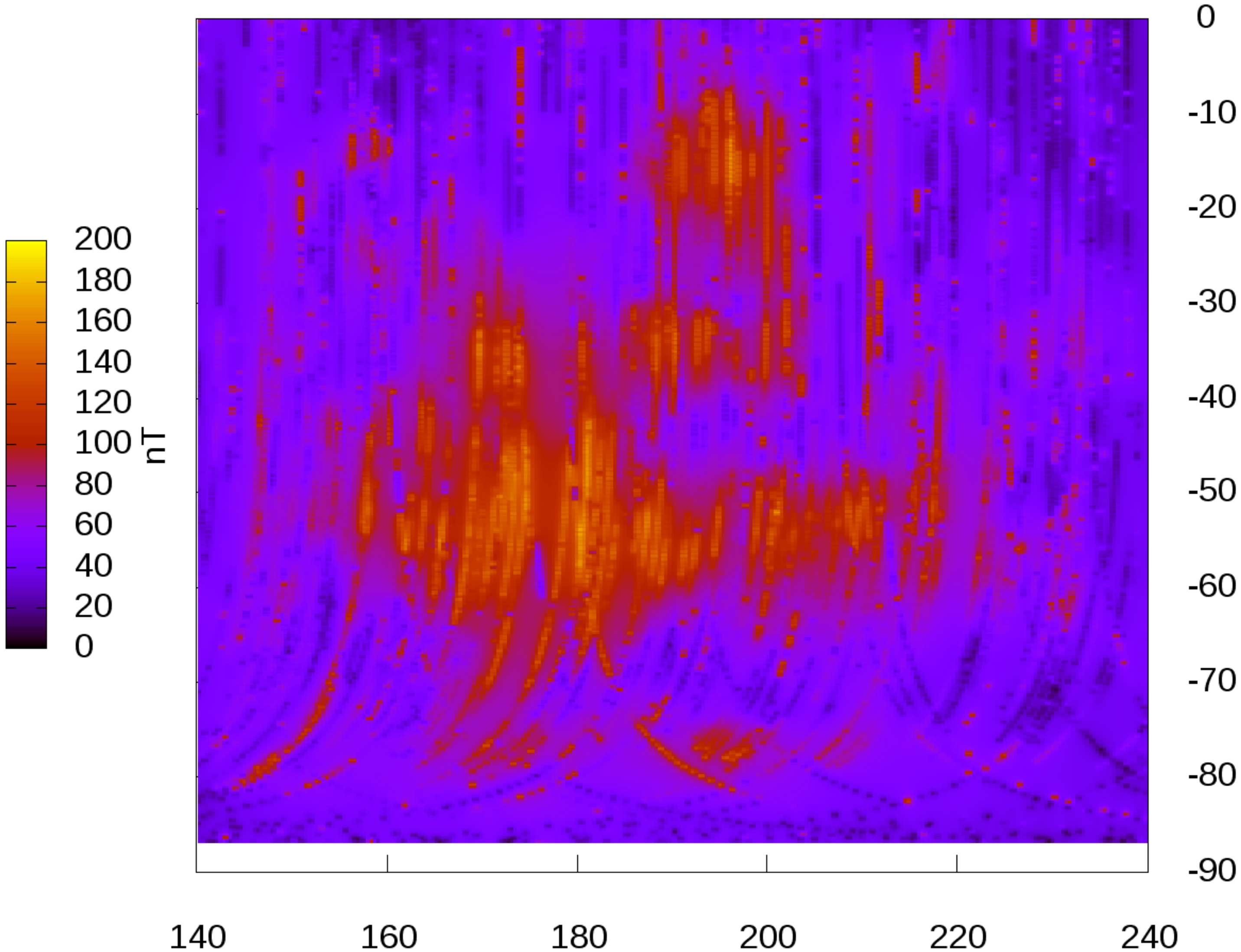

The measures depend on the height of the orbit, as is clearly seen in this zoomed region

Range of heights of the different orbits:

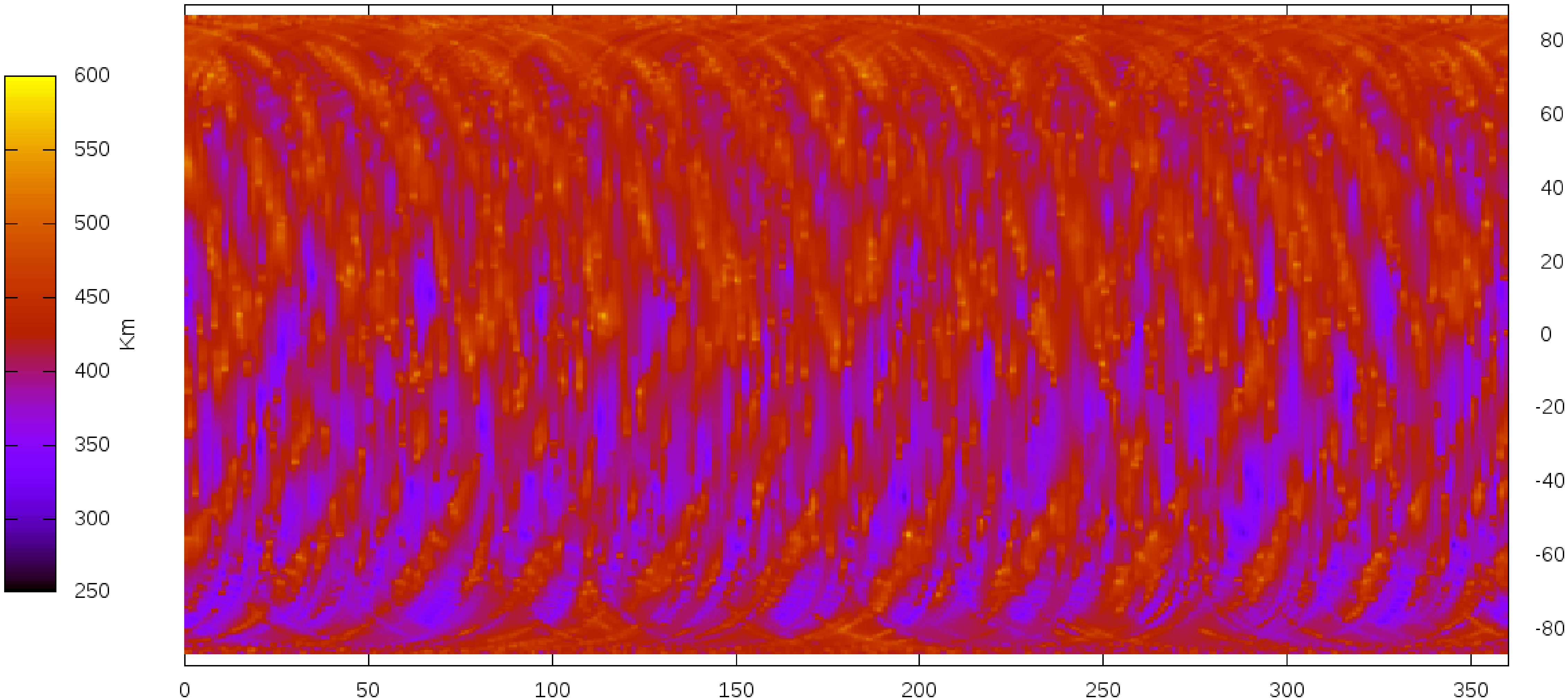

The same image from data form the Mars Global Surveyor Magnetometer/Electron Reflectometer (MAG/ER) (at $h = 3793.4$Km)

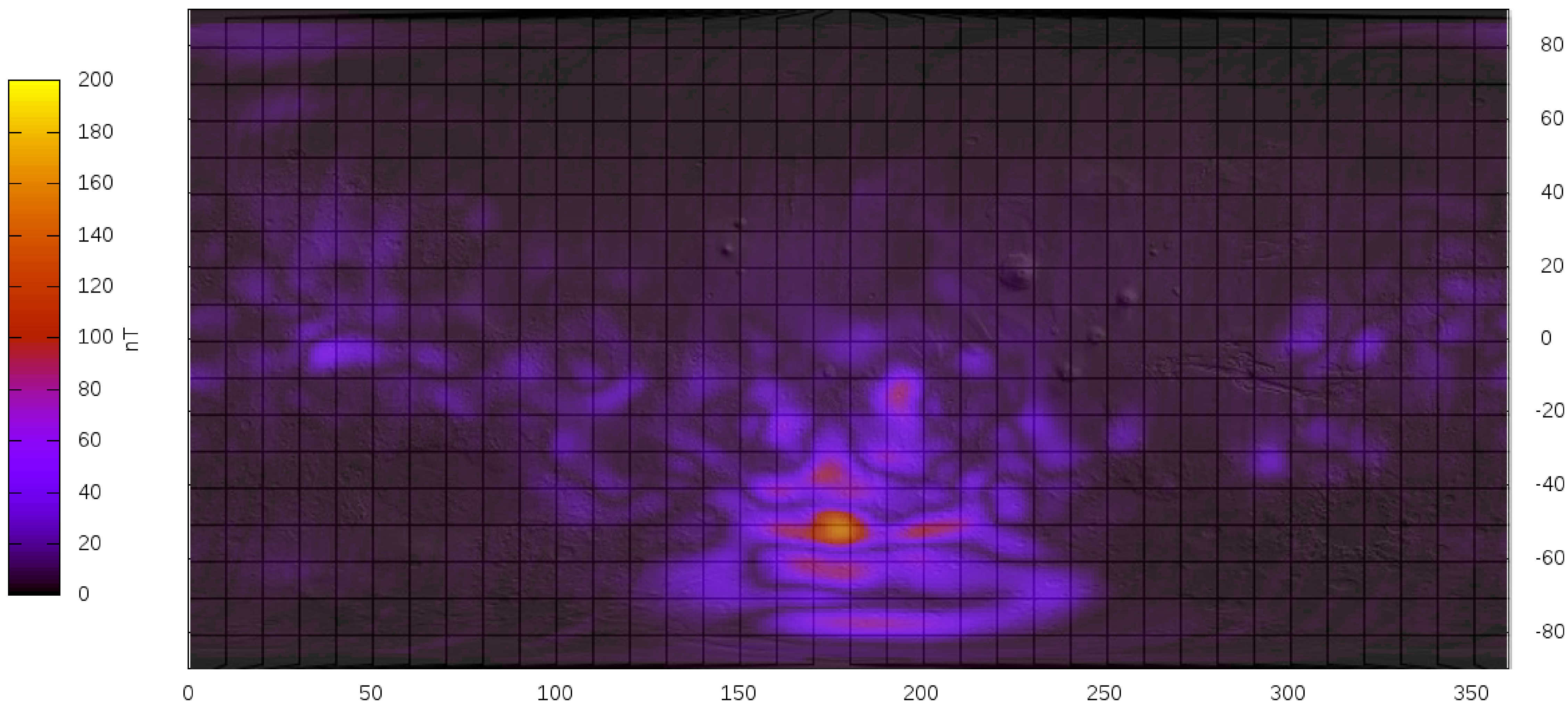

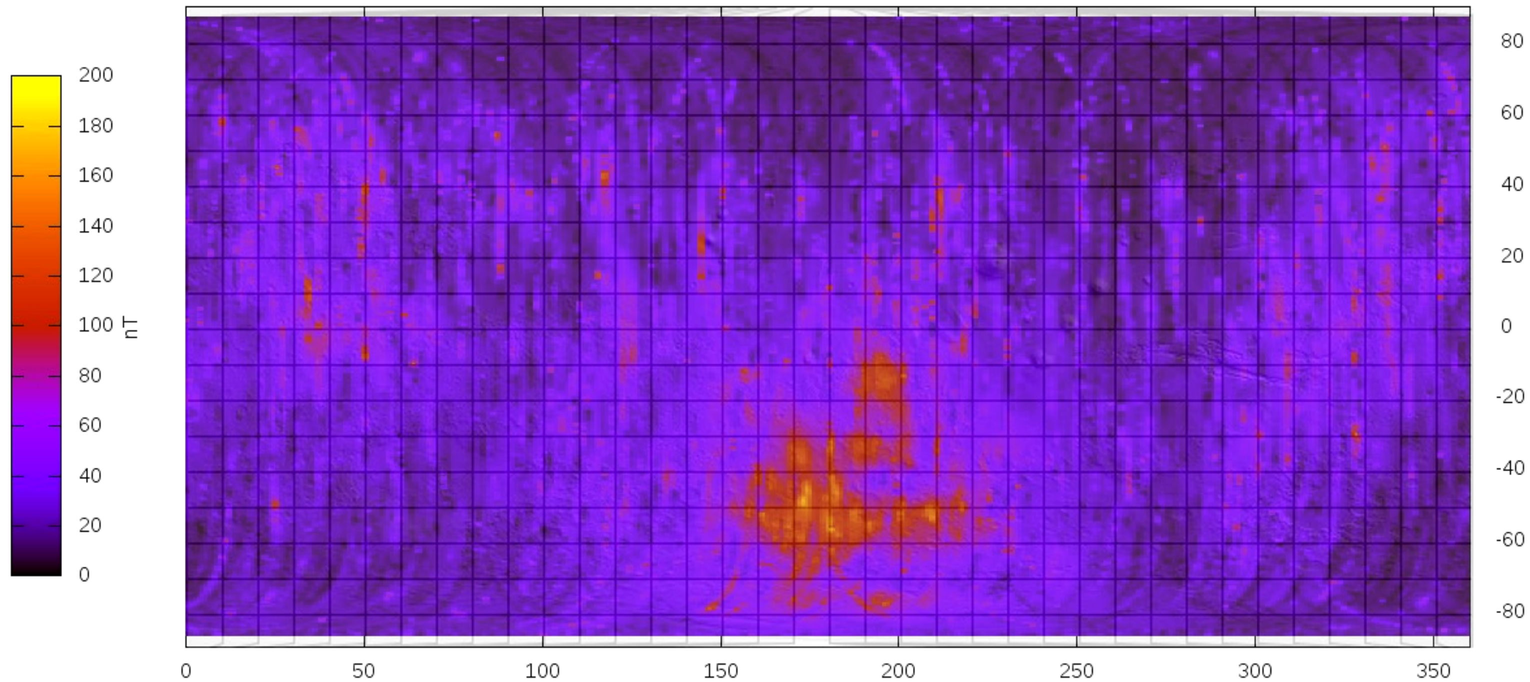

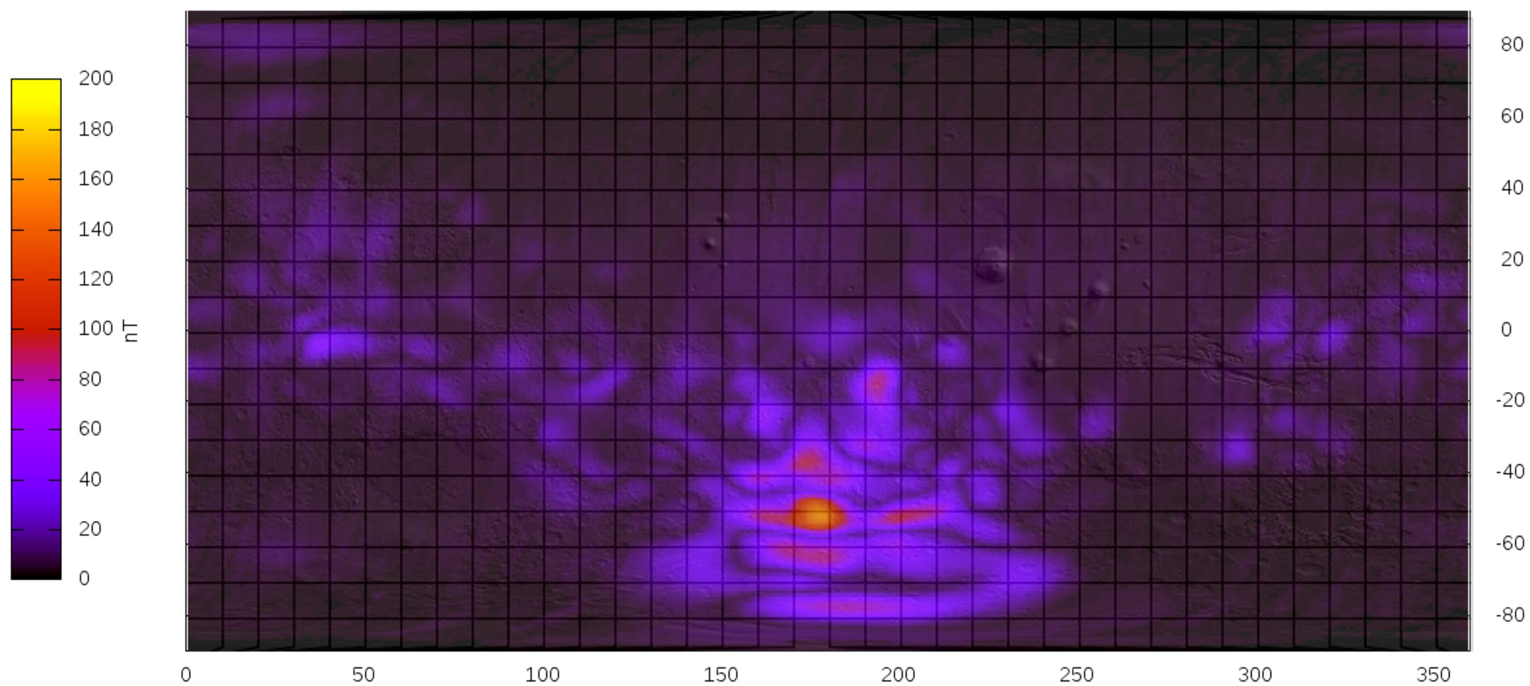

- The apparent discrepancies come from the different heights at which the measurements have been done.
- We are, presently, working on a way to estimate the radial magnetic field at a given altitude from MARSIS data.
- We are also analysing the existing methods that may provide the sign of the field.

Motion of a charged particle

• The non-relativistic motion of a charged particle in a magnetic dipole field is usualy refered to as the *Störmer Problem*.
• Particles with an energy below some threshold value are trapped in the field while more energetic particles can escape.
• Can be described by the two dimensional Hamiltonian system

$$H(\rho, z, \dot{\rho}, \dot{z}) = \frac{1}{2}\left(\dot{\rho}^2 + \dot{z}^2\right)^2 + \frac{1}{2}\left(\frac{1}{\rho} - \frac{\rho}{\left(\rho^2 + z^2\right)^{3/2}}\right)^2$$

• Nonintegrable and open to show chaotic behaviour [9].

⋆ The numerical study: • critically dependent on the method used.
• Standard methods show variations in the value of the energy, that may alter the actual boundedness/unboundedness of the solutions.
• Conservative and symplectic methods have been used to avoid this [5, 9].
• Avoid the cylindrical reduction and consider different field distributions [6, 7], keeping discrete conservation laws.

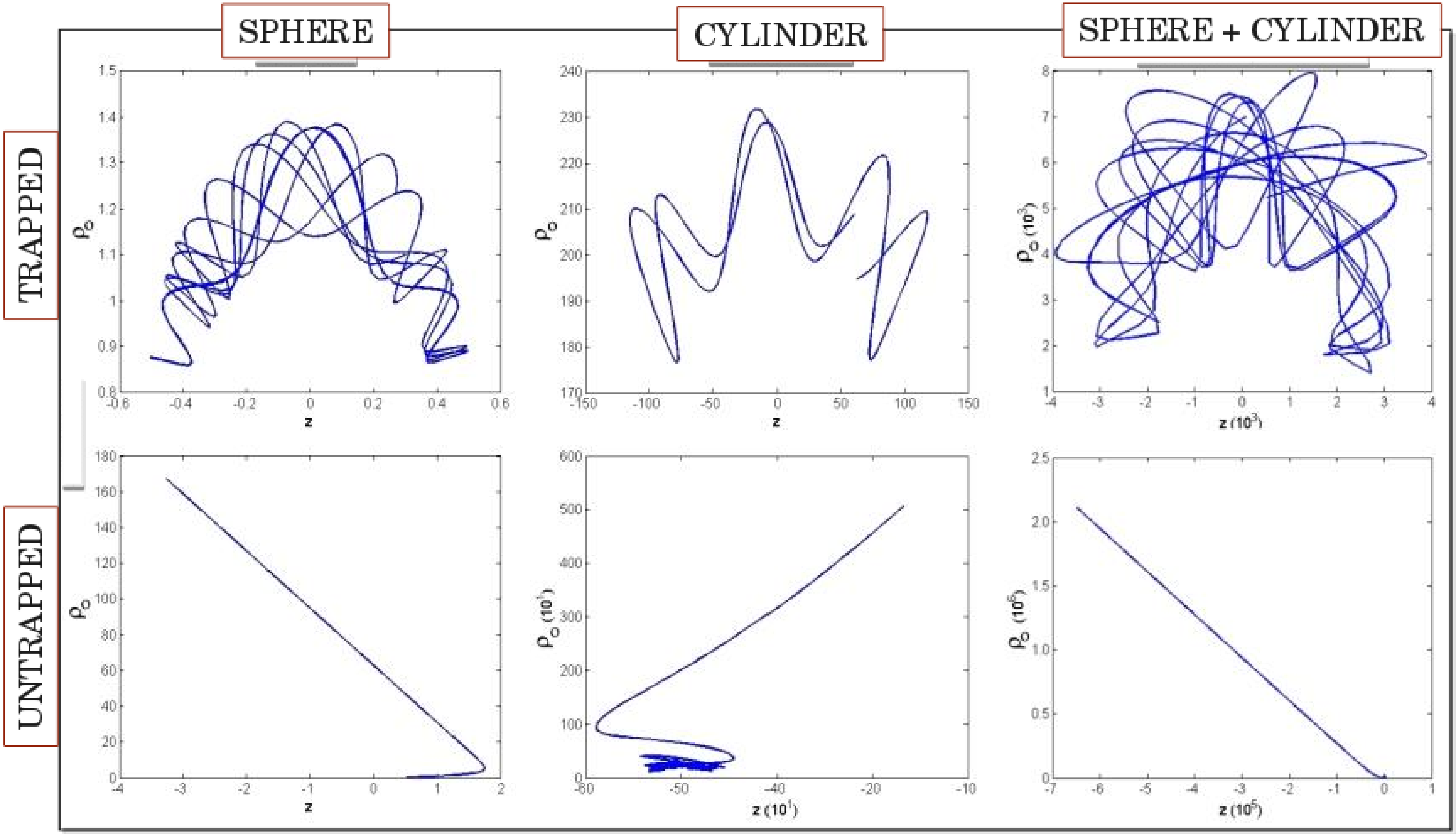

[Solutions in the general situation. Cartesian coordinates projected in cylindrical coordinates.[6]]

The degree of chaos of the solutions, both in the cylindrical reduction as well as in the general formulation, is an open problem that we are presently studying.

References

[1] R. Orosei, R.L. Jordan, D.D. Morgan, M. Cartacci, A. Cicchetti, F. Duru, D.A. Gurnett, E. Heggy, D.L. Kirchner, R. Noschese, W. Kofman, A. Masdea, J.J. Plaut, R. Seu, T.R. Watters, G. Picardi. "Mars Advanced Radar for Subsurface and Ionospheric Sounding (MARSIS) after nine years of operation: A summary", *Planetary and Space Science* **112** (2015), 9–114.

[2] M. Ramírez-Nicolás, B. Sánchez-Cano, O. Witasse, P.-L. Blelly, L. Vázquez. "The effect of the induced magnetic field on the electron density vertical profile of the Mars' ionosphere: A Mars Express MARSIS radar data analysis and interpretation, a case study", *Planetary and Space Science,* **126** (2016) 49–62.

[3] Sánchez-Cano, B., Witasse, O., Herraiz, M., Radicella, S.M., Bauer, J., Blelly, P.-L., Rodríguez-Caderot, G. "Retrieval of ionospheric profiles from the Mars Express MARSIS experiment data and comparison with radio occultation data", *Geoscientific Instrumentation, Methods and Data System* **1**, 1, 77–84, 2012.

[4] Akalin, F., Morgan, D.D., Gurnett, D.A., Kirchner, D.L., Brain, D.A., Modolo, R., Acuña, M.H., Espley, J.R. "Dayside induced magnetic field in the ionosphere of Mars", *Icarus* **206**, 104-111, 2010.

[5] Vázquez, L., and Jiménez, S. "Motion of a charge in a magnetic dipole field I. Painlevé, Analysis and a conservative numerical scheme", *Applied Mathematics and Computation* **25**, 207–217, 1988.

[6] María Ramírez-Nicolás, David Usero, Luis Vázquez, "Numerical studies of charged particles in a magnetic field: Mars application", *Central European Journal of Physics*, **12**(8), 521–531, 2014.

[7] M. Ramírez-Nicolás, D. Usero, M.P. Velasco, L. Vázquez, "Numerical study of a charged particle in a general magnetic field", *International Journal of Pure and Applied Mathematics*, **106** No.2, 401–414, 2016.

[8] Connerney et al., "The Global Magnetic Field of Mars and Implications for Crustal Evolution", *Geophysical Research Letters*, **28 (21)**, 4015–4018, 2001.
http:$//mgs-mager.gsfc.nasa.gov/publications/grl_28_connerney/$

[9] Rui Dilao and Rui Alves-Pires, Chaos in the Störmer Problem., *Progress in Nonlinear Differential Equations and Their Applications*, **75**, 175–194, 2007.

¡MUCHAS GRACIAS!

THANK YOU!